


Letter

# Associations between Benthic Cover and Habitat Complexity Metrics Obtained from 3D Reconstruction of Coral Reefs at Different Resolutions

Atsuko Fukunaga <sup>1,2,\*</sup> , John H. R. Burns <sup>3</sup>, Kailey H. Pascoe <sup>3</sup> and Randall K. Kosaki <sup>2</sup>

<sup>1</sup> Joint Institute for Marine and Atmospheric Research, University of Hawai'i at Mānoa, Honolulu, HI 96822, USA

<sup>2</sup> Papahānaumokuākea Marine National Monument, Office of National Marine Sanctuaries, National Ocean Service, National Oceanic and Atmospheric Administration, Honolulu, HI 96818, USA; randall.kosaki@noaa.gov

<sup>3</sup> Marine Science Department, University of Hawai'i at Hilo, Hilo, HI 96720, USA; johnhr@hawaii.edu (J.H.R.B.); kpascoe@hawaii.edu (K.H.P.)

\* Correspondence: atsuko.fukunaga@noaa.gov; Tel.: +1-808-725-5808

Received: 23 January 2020; Accepted: 16 March 2020; Published: 21 March 2020



**Abstract:** Quantifying the three-dimensional (3D) habitat structure of coral reefs is an important aspect of coral reef monitoring, as habitat architecture affects the abundance and diversity of reef organisms. Here, we used photogrammetric techniques to generate 3D reconstructions of coral reefs and examined relationships between benthic cover and various habitat metrics obtained at six different resolutions of raster cells, ranging from 1 to 32 cm. For metrics of 3D structural complexity, fractal dimension, which utilizes information on 3D surface areas obtained at different resolutions, and vector ruggedness measure (VRM) obtained at 1-, 2- or 4-cm resolution correlated well with benthic cover, with a relatively large amount of variability in these metrics being explained by the proportions of corals and crustose coralline algae. Curvature measures were, on the other hand, correlated with branching and mounding coral cover when obtained at 1-cm resolution, but the amount of variability explained by benthic cover was generally very low when obtained at all other resolutions. These results show that either fractal dimension or VRM obtained at 1-, 2- or 4-cm resolution, along with curvature obtained at 1-cm resolution, can effectively capture the 3D habitat structure provided by specific benthic organisms.

**Keywords:** photogrammetry; 3D reconstruction; digital elevation model; coral reef; structural complexity; curvature; habitat metric

## 1. Introduction

Scleractinian corals are ecosystem engineers that play an important role in coral reef ecosystems by providing a three-dimensional (3D) habitat structure that alters the physical environments and increases the availability of habitat for reef organisms [1]. High levels of live coral cover and 3D structural complexity are associated with higher abundances and diversity of reef organisms, although these effects may be site- and/or taxon-specific [2,3]. Coral growth forms also affect the distribution of reef fish, with morphologically complex corals (e.g., branching forms) supporting more diverse and abundant fish assemblages [4–6]. Quantifying the 3D habitat structure of coral reefs is, therefore, important when assessing the status of biological communities of coral reefs, as these data allow researchers to evaluate the effects of structural complexity on associated reef organisms [3].

In recent years, the health of coral reef ecosystems is increasingly threatened by various natural and anthropogenic stressors and disturbances, including extreme weather events, ocean acidification,

coral bleaching, *Acanthaster* (crown-of-thorns starfish) outbreaks, overfishing and urbanization [7–12]. In particular, the coral bleaching and subsequent (post-bleaching) mass mortality of corals can result in a radical shift in coral assemblages [11]. Corals exhibit differential responses to heat stress, with slow-growing species that possess simple morphologies often being more stress tolerant than fast-growing corals with branching and tabular growth forms [10,11]. Thus, bleaching events often result in a loss of morphologically complex corals and overall reef structural complexity [13]. These detrimental shifts in coral assemblage structure highlight the importance of continuous monitoring efforts that assess the status of coral reef communities and how changes in reef architecture affect the abundance and diversity of associated organisms.

The use of photogrammetric techniques has been gaining popularity in the 3D characterization of coral reef habitats as technological advancements in image sensors and data-processing capacity make the techniques more accessible and cost-effective [14–17]. Structure-from-motion (SfM) photogrammetry has been particularly useful for coral reef applications, because this range imaging technique estimates 3D structures from two-dimensional (2D) image sequences, which allows divers to use single lens imagery to create 3D reconstructions. Three-dimensional reconstructions of coral reef habitats generated using these technologies are then used to obtain data on the distribution of benthic organisms and/or metrics of habitat structure [18,19]. In our recent study examining the behavior of different habitat metrics extracted from digital elevation models (DEMs) derived from 3D reconstructions, several metrics that quantify the structural complexity of coral reefs, including fractal dimension, linear rugosity, surface complexity and slope, were all highly correlated [20]. On the other hand, curvature measures (profile and planform curvature) were uncorrelated to these metrics, indicating that these two types of metrics may complement one another when being used to characterize habitat structure [20]. As discussed in the same study, it is also important to consider the resolution of DEMs at which habitat metrics are extracted, as resulting values can be strongly influenced by the spatial resolution of the DEMs.

In the present study, we quantified multiple metrics of 3D structure from DEMs at different resolutions (i.e. raster cell sizes) and examined statistical associations between benthic cover and habitat complexity. The DEMs were extracted from 3D reconstructions of shallow ( $\leq 30$  m) coral reef habitats of the Northwestern Hawaiian Islands (NWHI). We focused on four metrics of structural complexity (fractal dimension, surface complexity, vector ruggedness measure (VRM) and slope) and two metrics of curvature (profile curvature and planform curvature). The main purpose of the study was to identify which taxonomic categories of living benthos, if any, were statistically associated with metrics of 3D habitat structure obtained at specific resolutions. This study offers valuable insights into how changes in the abundance and composition of benthic organisms affect the 3D architecture of coral reefs at different spatial resolutions. This information is important for coral reef monitoring programs, which typically focus on characterizing the 2D surface areas of live corals, as specific benthic organisms that disproportionately contribute to the overall 3D habitat structure can be identified.

## 2. Materials and Methods

### 2.1. Background

The present study was built on our previous work that investigated the behavior of different habitat metrics (including surface complexity, slope, VRM, fractal dimension, planform curvature and profile curvature) calculated from DEMs at 1-cm resolution, which were generated from 3D reconstructions of the same coral reef habitats in the NWHI [20]. The accuracy of the 3D models and the appropriateness of the choice of 1-cm resolution as the smallest size of raster cells (i.e. the highest resolution) were discussed in the previous work [20]. The use of DEMs, which project 3D models onto a 2D plane, thus resulting in the 3D structure being captured from above, was motivated by our effort to simplify both the process of image acquisition in the field to maximize the number of surveys and the post-survey analysis of resulting models to extract habitat metrics; we considered the loss of

information (e.g. overhangs associated with tabulate corals) resulting from capturing the reef habitat from a single projected overhead angle as an acceptable trade-off for a larger sample size [20]. The majority of geospatial analysis tools are still designed to process DEMs projected in 2.5 dimension rather than true 3D digital surface models [21], thus we used the DEM approach as this technique will be highly relevant to researchers until methods are developed that are capable of quantifying the same features from 3D digital surface models.

For the habitat metrics investigated in the present study, slope [21,22], VRM [21,23] and profile and planform curvature [24] are computed from the DEMs using the surface properties of the raster cells in  $3 \times 3$  windows. Slope and curvature are a gradient representing the first order derivative of the surface and the rate of change in slope, respectively, while VRM measures terrain ruggedness based on dispersion of vectors orthogonal to the surface. Surface complexity is calculated as the ratio of the 3D surface area along reef contours to the 2D planar area. Fractal dimension describes the irregularity of an object by combining information obtained at various spatial scales and is determined by changing the resolution of a DEM and measuring the 3D surface area at each of the resolutions, then inspecting the change in the 3D surface area at different resolutions [17].

## 2.2. Image Acquisition and Generation of 3D Models

The images of coral reefs were collected from islands/atolls of the NWHI during a Reef Assessment and Monitoring Program (RAMP) expedition aboard NOAA ship *Hi'ialakai* from September 6 to 30, 2017, under the conservation and management permit PMNM-2017-001A. Surveyed islands/atolls included French Frigate Shoals (Lalo;  $23^{\circ}52'N$ ,  $166^{\circ}17'W$ ), Laysan Island (Kamole;  $25^{\circ}42'N$ ,  $171^{\circ}44'W$ ), Lisianski Island (Kapou;  $26^{\circ}04'N$ ,  $173^{\circ}58'W$ ), Pearl and Hermes Atoll (Manawai;  $27^{\circ}56'N$ ,  $175^{\circ}44'W$ ), Midway Atoll (Kuaihelani;  $28^{\circ}12'N$ ,  $177^{\circ}21'W$ ) and Kure Atoll (Hōlanikū;  $28^{\circ}25'N$ ,  $178^{\circ}20'W$ ). Survey sites were randomly generated on bathymetric and bottom composition maps, in which targeted sites were hard-bottom habitat at depths within 0–30 m, using the geographic information system software ArcMap v.10.4 (Environmental Systems Resource Institute, Redlands, CA, USA). Weather conditions varied from day to day, but were mostly calm, with either sunny or cloudy skies throughout the expedition.

At each survey site, a pair of SCUBA divers laid a 30-m transect line along a bathymetric depth contour and collected overlapping imagery along the transect line, aiming for 70%–80% overlaps between images. Divers first placed a ground control point (GCP) unit at one end of the transect line. The GCP unit had coded targets on scale bars to enable accurate georeferencing of the survey sites (Figure S1). Divers then manually took each image using the single shooting setting, while swimming slowly above each side of the transect line at approximately 2–3 m above the substrate, aiming to cover approximately  $90\text{-m}^2$  (30-m length  $\times$  3-m width) area. All photographs were taken using a Canon EOS Rebel SL1 digital SLR camera with an 18–55 mm lens in an Ikelite housing with a 6-inch dome port. The focal length of 18 mm was used throughout the process of image collection, with a shutter speed of 1/250 second, an aperture of f/10 and an auto ISO.

Three-dimensional models of survey sites were constructed from the imagery using the software Agisoft PhotoScan Professional v.1.4 (Agisoft LLC., St. Petersburg, Russia), as reported in Fukunaga et al. [20]. Camera calibration and optimization were completed using the PhotoScan software. The software performs calibration using Brown's distortion model and is capable of resolving the optical characteristics of the camera lens directly from the image metadata without prior calibration. Pre-calibration of the camera in the surveyed environment is desirable, but was not practical for this study due to time and equipment constraints associated with working in this remote location. The capability of the software to resolve the optical characteristics of the lens without prior calibration enabled us to process the overlapping imagery without the time-consuming process of pre-calibration. A sparse 3D point cloud was generated through the photoalignment process in the software and the known  $x$ ,  $y$ ,  $z$  coordinates of the coded targets on the GCP unit were used to create a local coordinate system. After self-calibrating bundle adjustment using the GCP reference coordinates, a dense point

cloud was produced. An orthophotomosaic and a DEM were then generated and exported for each survey site as GeoTIFF elevation data files with local coordinates for further processing in the CoralNet website ([coralnet.ucsd.edu](http://coralnet.ucsd.edu)) [25] and the statistical software R v.3.5.3 [26], respectively (Figure S2). The process was completed on either an Intel Xeon workstation with a 32GB RAM and FirePro W5100 GPU or Intel Core i7 laptops with a 64GB RAM and GeForce GTX 980 GPU. Ground sampling distances of the resulting 3D models ranged from 0.00026 to 0.00084 meter/pixel, with errors of 0.5–2.3 pixels [20].

### 2.3. Estimation of Live Coral Cover and Habitat Metrics

Orthophotomosaics were uploaded to the CoralNet website to estimate benthic cover for all survey sites. For each orthophotomosaic, 1000 random points were generated by the website and each point was annotated by identifying a benthic taxon or abiotic feature under the point. Live coral was classified down to the genus level and associated morphology. While CoralNet allows for fully- or partially automated annotation through its machine-learning algorithms, this function was not used in the present study. All annotations were completed manually without machine-learning tools. In order to ensure the accuracy and consistency of annotation, a single expert coral biologist trained all annotators, and the same coral biologist reviewed annotations for quality control. The proportion of each benthic category was obtained for each site by dividing the number of points for each category by the total number of random points after removing the points that happened to fall on a transect line, mobile vertebrates (i.e., fish), or any other unidentifiable objects.

Digital elevation models were exported at 1-cm resolution (i.e. 1-cm  $\times$  1-cm raster cell size) and processed in R using the *sp* [27,28], *raster* [29] and *rgeos* [30] packages. The *aggregate* function in the *raster* package was used to change the raster cell resolutions of the DEMs from 1 cm to 2, 4, 8, 16 and 32 cm. Surface complexity, slope, VRM and profile and planform curvature were computed from the DEMs at each resolution (Figure S2). These metrics, with the exception of surface complexity, were calculated for each raster cell of a DEM so we averaged values from all the cells in order to obtain a single representative value of these metrics for each DEM. Fractal dimension ( $D$ ) was calculated as  $D = 2 - \text{slope} \log S(\delta) / \log(\delta)$ , in which  $\delta$  was a resolution of the DEM (i.e., 0.01, 0.02, 0.04, 0.08, 0.16 or 0.32 m) and  $S(\delta)$  was the 3D surface area at the given resolution  $\delta$  [17]. Note that surface complexity, slope, VRM, profile curvature and planform curvature were calculated for each of the six resolutions examined while fractal dimension would result in a single value for the range of the six resolution, as fractal dimension represents how 3D surface area changes over a given range of spatial resolution (i.e. 0.01–0.32 m). The upper limit of 32-cm resolution was chosen based on the total area of each DEM and the fact that some of the metrics (i.e. slope, VRM and profile and planform curvature) required  $3 \times 3$  windows for calculation.

### 2.4. Statistical Analyses

Analyses of benthic cover and habitat metrics were done using R statistical software, with the *nlme* [31] and *car* [32] packages for model building and validation. We fitted each habitat metric obtained at each of the six different resolutions to the sum of terms in benthic cover after considering the following four different structures of the random component: (Model 1) a general linear model with the assumption of equal variance, (Model 2) a generalized least squares model allowing for the spread of the residuals to vary per island/atoll, (Model 3) a mixed effects model that included the island/atoll term as a random effect, and (Model 4) a mixed effects model that included the island/atoll term as a random effect and also allowing for the spread of the residuals to vary per island/atoll. We considered these four structures as the islands/atolls of the NWHI support different varieties of habitat types. The selection of the random structure was based on the Akaike's Information Criterion (AIC). The backward elimination procedure followed to select fixed terms (i.e. benthic cover) based on the  $t$ -statistic at  $\alpha = 0.05$ . After the model selection procedure, standardized residuals were plotted against all eliminated explanatory variables and if any clear patterns were found, those terms were added back to the model and re-evaluated.

The fixed terms considered in each model were different morphologies of corals (see Results for details), algae, crustose coralline algae (CCA), hard substrates (with or without growth of turf algae) and rubble. We used morphologies, rather than combinations of coral genera and morphologies, because separating corals into genera and morphologies resulted in sparse data for some genus/morphology combinations, and also because the actual coral morphologies are more likely to affect 3D habitat metrics than the taxonomic identity of corals. Other invertebrates, such as bivalves, tunicates and zoanthids, were excluded from the analysis, as they never contributed to more than 1% of benthic cover at any of the survey sites. After fixed terms were selected for each model, the variance inflation factor was calculated for each term to evaluate for multicollinearity.

A pseudo  $R^2$  value was calculated for each selected model as a reference in order to quantify the amount of variability in 3D habitat structure explained by benthic cover:  $\text{pseudo } R^2 = 1 - \frac{\sum(Y - \hat{Y})^2}{\sum(Y - \bar{Y})^2}$  where  $Y$  is the observed value,  $\hat{Y}$  is the fitted value, and  $\bar{Y}$  is the mean of all observed values. For selected models that included the island/atoll term as a random term (i.e. Models 3 and 4), their pseudo  $R^2$  values also included the effects of the island/atoll term. We calculated a pseudo  $R^2$  value without any fixed terms (i.e. benthic cover), so that the amount of variability explained by the selected model could be compared with the amount of variability solely explained by the island/atoll term, allowing for the estimation of the amount of variability explained by benthic cover.

### 3. Results

In total, 80 shallow forereef sites with depths ranging from 1 to 26 m were surveyed using photogrammetric techniques during the RAMP expedition; 25 sites were completed at French Frigate Shoals, 10 sites at Laysan Island, 15 sites at Lisianski Island, 15 sites at Pearl and Hermes Atoll, 9 sites at Midway Atoll and 6 sites at Kure Atoll. The total live coral cover varied among these islands/atolls, with Lisianski Island having the highest median cover of 20.3% (25%–75% quantile range = 11.4%–39.8%), followed by 19.4% (6.7%–52.8%) at French Frigate Shoals, 4.2% (2.3%–5.1%) at Kure Atoll, 2.5% (0.5%–17.1%) at Laysan Island, 2.0% (1.2%–2.4%) at Midway Atoll and 0.9% (0.2%–3.6%) at Pearl and Hermes Atoll.

Eleven combinations of coral genera and growth morphologies were identified in the present study: branching *Acropora*, tabulate (table-shaped) *Acropora*, encrusting *Montipora*, foliose *Montipora*, encrusting *Pavona*, mounding *Pavona*, branching *Pocillopora*, branching *Porites*, encrusting *Porites*, foliose *Porites* and mounding *Porites*. Encrusting *Pavona* and mounding *Pavona* were only present at four sites and contributed to less than 0.4% of the benthos at each site. *Montipora* was also never highly abundant; encrusting *Montipora* and foliose *Montipora* occurred at 27 and 8 sites, respectively, with a maximum percent cover of 12% for both growth forms, with foliose *Montipora* always co-occurring with encrusting *Montipora*. Similarly, foliose *Porites* occurred at five sites, never comprising more than 1% of the benthos at any of the sites, and always co-occurred with encrusting *Porites*. Thus, these corals were separated into four different morphologies: tabulate, branching, encrusting and mounding (Table 1).

**Table 1.** Summary of coral morphologies used in the data analysis and coral genera and growth forms included in each morphology.

Morphology	Growth Forms and Genera
tabulate	tabulate <i>Acropora</i>
branching	branching <i>Acropora</i> , branching <i>Pocillopora</i> , branching <i>Porites</i>
encrusting	encrusting <i>Montipora</i> , encrusting <i>Porites</i> (rare: foliose <i>Montipora</i> , foliose <i>Porites</i> , encrusting <i>Pavona</i> )
mounding	mounding <i>Porites</i> (rare: mounding <i>Pavona</i> )



Fractal dimension obtained from the range of 1- to 32-cm resolutions was very strongly correlated (sample correlation coefficient:  $|r| > 0.80$ ), with surface complexity and slope at 1- and 2-cm resolutions, as well as with VRM at 1-, 2-, 4- and 8-cm resolutions (Figure 1). These correlations decreased at lower resolutions, reaching values of approximately 0.2 for surface complexity and slope and 0.3 for VRM at 32-cm resolution. The two curvature measures had very weak correlation ( $|r| < 0.2$ ) with fractal dimension when computed at 1- or 2-cm resolution, and those computed at lower resolutions ( $\geq 4$  cm) mostly had weak negative correlations (Figure 1).

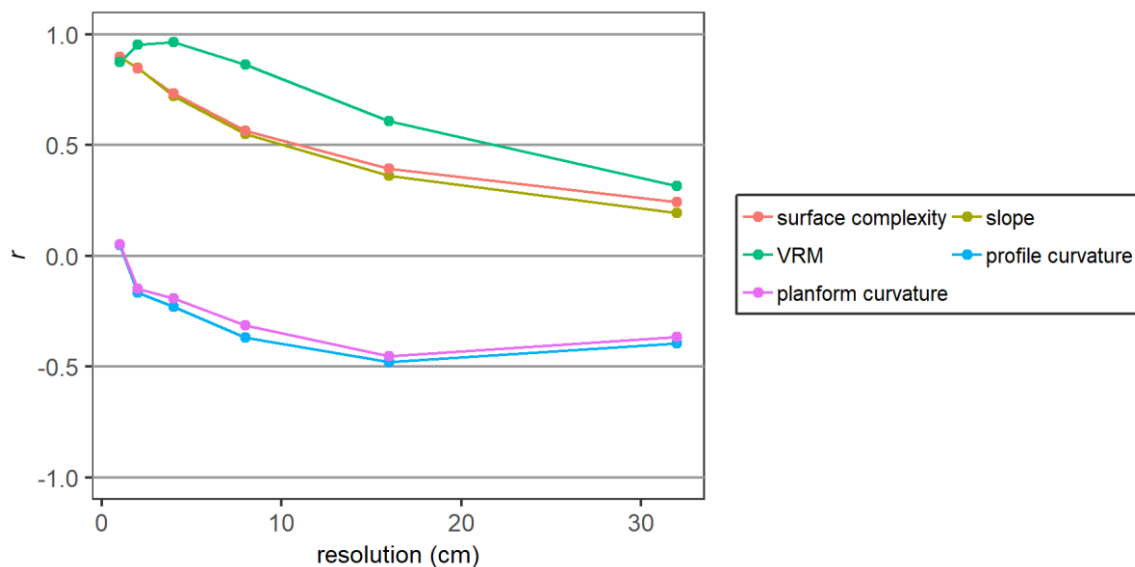


**Figure 1.** Sample correlation coefficient ( $r$ ) between fractal dimension obtained for the range of 1- to 32-cm resolution and other structural complexity metrics (surface complexity, slope and vector ruggedness measure (VRM)) and curvature measures (profile curvature and planform curvature) at 1-, 2-, 4-, 8-, 16- and 32-cm resolutions.

Surface complexity and slope obtained at 1-cm resolution were very strongly correlated with one another, and the very strong correlation between these two metrics of structural complexity was maintained at the lower resolutions of 2, 4, 8, 16 and 32 cm (Figure 2a,b). Similarly, VRM had strong positive correlations ( $0.6 \leq r \leq 0.8$ ) with surface complexity and slope at 1-, 2-, 4- and 8-cm resolutions and very strong positive correlations ( $r > 0.8$ ) at 16- and 32-cm resolutions (Figure 2c). The two curvature measures generally had very weak to moderate correlations ( $|r| < 0.6$ ) with the three metrics of structural complexity, with the exception of profile curvature and VRM at 16-cm resolution (Figure 2).

Profile curvature and planform curvature values had  $r \approx 1$  at 1-cm resolution, and their correlation was above 0.94 at 2-, 4- and 8-cm resolutions (Figure 3). Their correlation decreased to 0.82 at 16-cm resolution and was 0.57 at 32-cm resolution (Figure 3). As previously mentioned, correlations between curvature and complexity metrics were mostly below 0.6 (Figures 2 and 3), and overall, slope was least correlated with both curvature measures among the three metrics of structural complexity (Figures 2b and 3).

The best structure of the random component based on AIC almost never included the island/atoll term as a random effect (i.e. Model 1 or Model 2) for the metrics of structural complexity, but it was the opposite for the curvature measures where including the island/atoll term as a random effect (i.e. Model 3 or Model 4) almost always resulted in lower AIC values. The exceptions were VRM at 2-cm resolution and slope at 16-cm resolution for the metrics of structural complexity, and planform curvature at 8-cm resolution and 32-cm resolution for curvature. For all of the exceptions, the differences in AIC values were less than 0.5, indicating that the inclusion or exclusion of the random effect made little improvement to these models. In addition, the AIC value for profile curvature at 32-cm resolution was

the lowest using Model 1, followed by Model 3. Their difference in AIC were  $\approx 2$ , and the selected fixed terms using these two models were the same. We thus chose to not include the random effect in the final models for the metrics of structural complexity, while including it in all the models for the curvature measures (Tables A1 and A2 in Appendix A).

Despite the high correlations among the metrics of structural complexity, the selected fixed terms in the final models for these metrics slightly differed (Table A1). A general pattern was, however, that these metrics were positively correlated with proportions of branching, encrusting and mounding corals and CCA at relatively high resolutions. In particular, the most structurally complex branching morphology had a statistically significant positive correlation when habitat metrics were obtained at 1-cm resolution for surface complexity, 1- and 2-cm resolutions for slope and 1-, 2- and 4-cm resolutions for VRM. The amount of variability explained by benthic cover (i.e. pseudo  $R^2$  values) quickly decreased towards lower resolutions (Figure 4). The metric VRM was slightly different from either surface complexity or slope, in that the highest pseudo  $R^2$  value was observed at 2-cm resolution and pseudo  $R^2$  remained relatively high, even at 4-cm resolution. Vector ruggedness measure at 4-cm resolution and fractal dimension were also the only metrics that were positively correlated with tabulate coral cover (Table A1). Similarly, slope metrics at 1-, 2- and 4-cm resolutions were the only ones that had positive correlations with hard substrates.

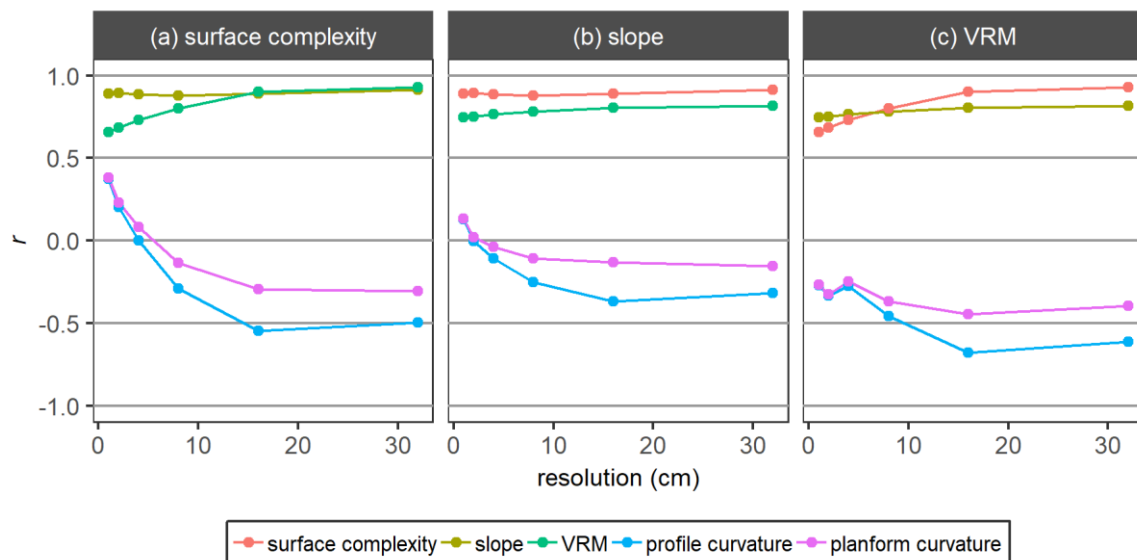


**Figure 2.** Sample correlation coefficient ( $r$ ) between the three metrics of structural complexity ((a) surface complexity, (b) slope and (c) VRM) and other habitat metrics. All metrics were obtained at 1-, 2-, 4-, 8-, 16- and 32-cm resolutions, and the correlation coefficients were for metrics obtained at the same resolution.

Profile and planform curvature measures had, as expected from the very high correlation between them, the same final models when obtained at 1-, 2-, 4- and 8-cm resolutions (Table A2). These curvature measures were positively correlated with proportions of mounding corals and CCA and negatively correlated with branching coral cover at 1-cm resolution, and also negatively correlated with branching coral cover at 2-cm resolution (Table A2). There were no benthic categories that had a statistically significant correlation with these measures at either 4- or 8-cm resolution. At 16- and 32-cm resolutions, profile curvature was negatively correlated with mounding coral cover, while planform curvature was positively correlated with proportions of algae and hard substrates at 16-cm resolution and additionally with branching corals at 32-cm resolution. Planform curvature at 32-cm resolution was also negatively correlated with mounding coral cover. Note that the amount of variability explained by benthic cover after accounting for the effects of islands/atolls was generally very low (pseudo  $R^2 < 0.1$ ) for curvature measures obtained at all resolutions, except for 1 cm (Figure 5).

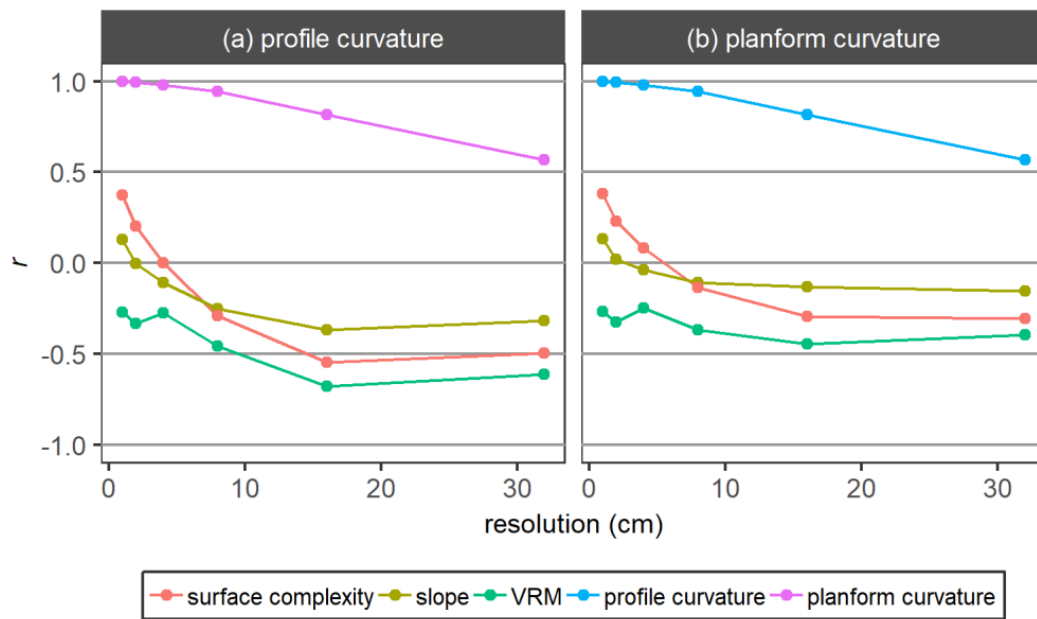


**Figure 3.** Sample correlation coefficient ( $r$ ) between the two curvature measures, (a) profile curvature and (b) planform curvature, and other habitat metrics. All metrics were obtained at 1-, 2-, 4-, 8-, 16- and 32-cm resolutions, and the correlation coefficients were for metrics obtained at the same resolution.

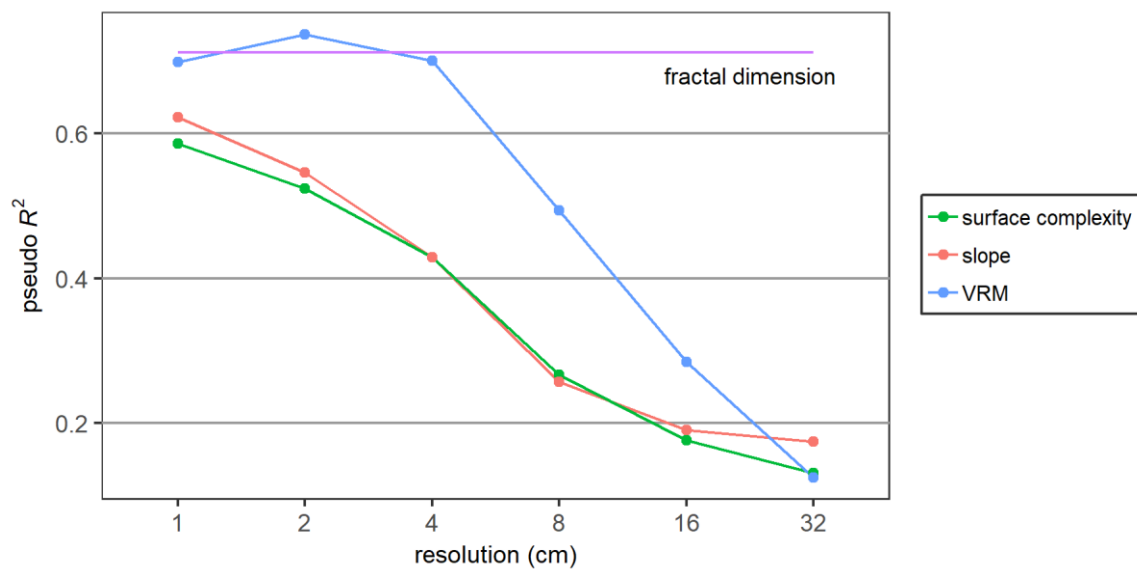


**Figure 4.** Pseudo  $R^2$  values for the selected models for the complexity metrics, surface complexity, slope and VRM, at 1-, 2-, 4-, 8-, 16- and 32-cm resolutions. One for fractal dimension for the range of 1- to 32-cm resolutions is shown as a horizontal line.



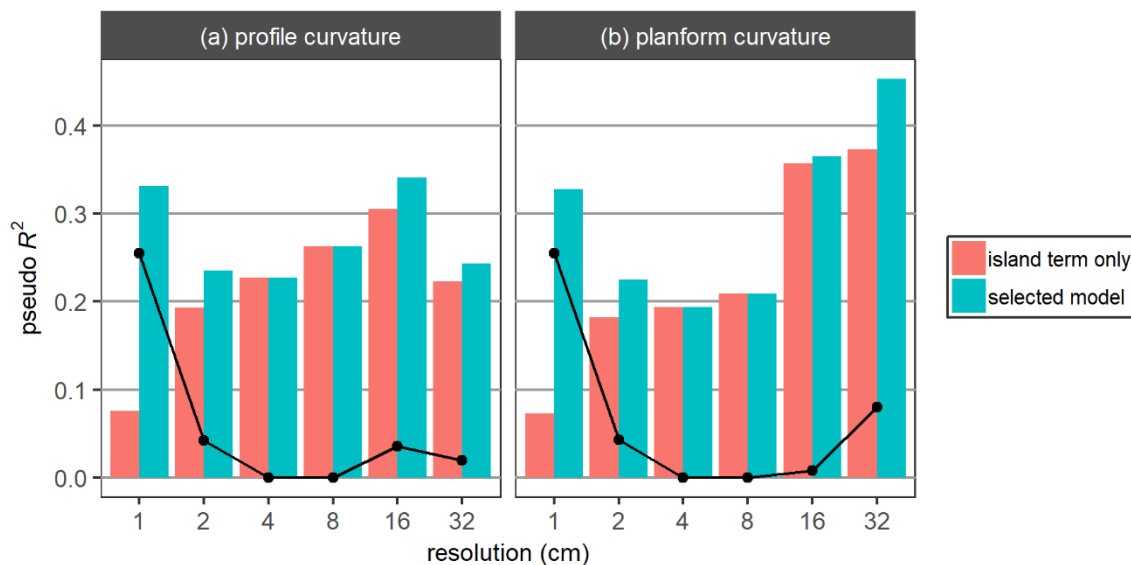


**Figure 5.** Pseudo  $R^2$  values for the selected models and models only with the island term fitted as a random effect (i.e. no fixed terms) for (a) profile curvature and (b) planform at 1-, 2-, 4-, 8-, 16- and 32-cm resolutions. Unlike the metrics of structural complexity, the selected models for curvature included the islands/atoll term as a random effect. The amount of variability explained by selected fixed terms was, therefore, estimated by subtracting the pseudo  $R^2$  value for the island term only from the pseudo  $R^2$  value for the selected model, and is shown here with a black line.

#### 4. Discussion

The study presented here examined relationships between benthic cover on coral reefs in the NWHI and four metrics of 3D habitat structural complexity (fractal dimension, surface complexity, slope and VRM) and the two curvature measures (profile curvature and planform curvature) obtained at six different resolutions, ranging from 1 to 32 cm. For the complexity metrics, there was an overall pattern in how associations between benthic cover and these metrics changed as the resolutions increased/decreased. Structurally complex branching coral cover was correlated with the complexity metrics at higher resolutions (raster cell size  $\leq 4$  cm), and the amount of variability in the complexity metrics explained by benthic cover quickly decreased as the resolution decreased. There were also slight differences in terms of which benthic categories had statistically significant correlations with the metrics of structural complexity. The amount of variability in the curvature measures explained by the categories of benthic cover was generally very low, with the exception of those obtained at 1-cm resolution where branching and mounding coral cover and CCA had statistically significant correlations with profile and planform curvature.

Fractal dimension has been previously suggested as a reliable measure of coral morphology using *Pocillopora*, *Acropora* and *Porites* [33]. While the range of resolution in that study was much smaller (0.3 mm–10 cm) than the present study, our result indicates that the fractal dimension obtained using the range of resolutions from 1 to 32 cm also captures the morphological complexity of branching, mounding, encrusting and tabulate corals, as well as CCA. The selected model for fractal dimension explained a larger amount of variability (pseudo  $R^2 = 0.712$ ) in this metric than those for surface complexity or slope at any of the examined resolutions (Figure 4). Fractal dimension combines information obtained at various spatial scales (1 to 32 cm in our case), and while applying the concept of fractal dimension to quantifying the surfaces of coral heads or colonies [33,34] or to estimating the structural complexity of coral reefs [17,35] is not new, our results demonstrate that this multiscale metric obtained from DEMs is superior to either surface complexity or slope in terms of capturing the structural complexity of reef organisms.

The final model for surface complexity obtained at 1-cm resolution included a similar set of fixed terms where the only difference from fractal dimension was the exclusion of tabulate coral cover.

The amount of variability explained by the fixed terms was much smaller for surface complexity than fractal dimension (Figure 4). This was somewhat surprising, as fractal dimension in the present study was essentially the rate of change in surface complexity from 1- to 32-cm resolutions in a logarithmic scale. Surface complexity measures spatial heterogeneity or rugosity using the ratio of actual surface area and its horizontal projection (i.e. 2D planar area) and is often measured using the chain-and-tape method in coral reef environments [36,37]. The importance of considering spatial scales at which rugosity is estimated on coral reefs has been previously examined by using different sizes of chain links [37]. Here, we considered different spatial scales by using six different resolutions, and the highest resolution (i.e. the smallest spatial scale of 1 cm.) worked best in capturing the structural complexity of benthos. While surface complexity adequately characterizes habitat structure at 1-cm resolution, the fractal dimension value that integrates surface complexity from all six resolutions provides an even better metric to quantify habitat structure.

Slope was the only metric of structural complexity that had a positive correlation with the proportion of hard substrates. Although slope and surface complexity had very strong correlations with one another at all resolutions in the present study, these two metrics quantify different structures. Slope is the measure of steepness and is calculated for each cell of a DEM, based on the surface properties of  $3 \times 3$  neighboring cells [21], while surface complexity is a measure of rugosity as described above. Despite the very strong correlations, the mechanisms by which these two metrics increase when benthic organisms add 3D structure to a substrate are different. Surface complexity increases due to an increase in the 3D surface area, while slope increases as the 3D structure creates grades. These metrics are also affected by the surface topography of the substrate itself. Slope can increase due to relatively gentle grades created by bare substrates while surface complexity may not increase as much since an increase in the 3D, compared to 2D, surface area by such grades is unlikely to be large. Examining detailed properties of these two metrics is beyond the scope of this study, but a further investigation that utilizes simulated surfaces should reveal how each metric responds to changes in surface topography of bare substrate and potentially separate their uses in quantifying the habitat structure of coral reefs.

Unlike surface complexity and slope, VRM had relatively high pseudo  $R^2$  values at 1-, 2- and 4-cm resolution, with the highest value at 2-cm resolution. This metric measures the dispersion of normal vectors using a  $3 \times 3$  neighboring cell window of a DEM. The elevation value contained in each cell of a DEM generates a surface with slope and aspect (i.e. slope direction), and the normal vector is a vector orthogonal to this surface [23]. Thus, VRM quantifies the variability in the directions where each surface is facing. Considering the structural characteristics captured by VRM, this metric seems most interpretable in relation to coral morphologies. Vector ruggedness measure was positively correlated with branching coral cover at 1-, 2- and 4-cm resolutions, and encrusting coral cover at 1-, 2-, 4- and 8-cm resolutions (Table A1). On the other hand, it was positively correlated with mounding coral cover at 4-, 8- and 16-cm resolutions (Table A1). It is also interesting to note the positive correlation with tabulate coral cover at 4-cm resolution (Table A1). Although tabulate corals in the NWHI (predominantly *Acropora cytherea*) have a fine-scale structure including small branches and tube-like corallites, such a fine-scale structure is often not captured in a DEM using a cell size of  $\geq 1$  cm. Thus, the correlation at 4-cm resolution is likely due to the drop from a tabletop to either another layer or a surrounding substrate, not the fine-scale structure of *A. cytherea*. In addition, while this is not a matter limited to VRM, habitat created under these table-shaped corals is not perfectly captured in DEMs, as they are rendered from an overhead “bird’s-eye view” planar graphical projection. This has an important implication and requires caution when using any habitat metrics extracted from a DEM for ecological studies, as some organisms utilize this space (e.g. *Lutjanus kasmira* in the NWHI [38]). Nevertheless, the relatively high values of pseudo  $R^2$  and the interpretability in relation to coral morphology make VRM obtained at 1-, 2- or 4-cm resolution suitable for quantifying the structural complexity of coral reefs.

Curvature measures the rate of change in the gradient and direction of slope; profile curvature measures curvature in the direction parallel to the slope and planform curvature in the direction

perpendicular to the slope [24]. For profile curvature, negative and positive values indicate that the surface is upwardly concave and upwardly convex, respectively, and for planform curvature, negative and positive values indicate that the surface is laterally convex and laterally concave, respectively [24,39]. Both curvature measures exhibited positive correlations with mounding coral cover and CCA cover at 1-cm resolution (Table A2), which indicates increases in upward convexity and lateral concavity with increases in mounding coral or CCA cover. The negative correlations with branching corals (Table A2) indicate the opposite: increases in upward concavity and lateral convexity with increases in branching coral cover. While this seems to be consistent with the morphology of these benthic organisms, the overall variability in the curvature measures that was explained by the proportion of these benthic categories was relatively small (Figure 5), indicating that there are potentially other factors affecting curvature. This is consistent with the structure of the random component for model selection where, unlike the complexity metrics, including the island/atoll term as a random effect was almost always the best option for modeling these curvature measures. A closer inspection of curvature values obtained at different resolutions shows that most curvature values in the present study were negative, and they regressed to zero (i.e. the surfaces were horizontal) as resolutions decreased and the surface of the 3D models flattened (Figure 6). In addition, 3D models with positive profile and planform curvature values at 1-cm resolution all seem to have small ledge-like structure or holes on the reefs, suggesting that surface topography, rather than benthos, may have a stronger effect on values of curvature. Similar to the case of slope, a further investigation utilizing simulated surfaces should clarify how surface topography affects curvature and how these effects compare to those of benthic compositions.

Coral reef monitoring programs often characterize benthic habitat through the use of photo-quadrats and subsequent image annotation that quantifies the 2D surface area of live corals. Our study presented here clearly demonstrates how such information of a 2D surface area can be translated into 3D habitat complexity by quantifying the contribution of each type of coral morphology to specific structural metrics. Conversely, the ability to identify different habitat metrics that capture relative abundances of specific benthic organisms or their morphologies has important implications for continuous efforts of monitoring programs. As manual annotation of benthic imagery is very time-consuming and requires a large amount of human effort, eliminating this process means the potential to reallocate the limited resource to other areas of monitoring programs. As the health of coral reef ecosystems is increasingly threatened [7–12], the need for continuous monitoring efforts also increases. Time-efficient survey and post-survey processing protocols that utilize the photogrammetric techniques described here can greatly enhance coral reef monitoring programs.

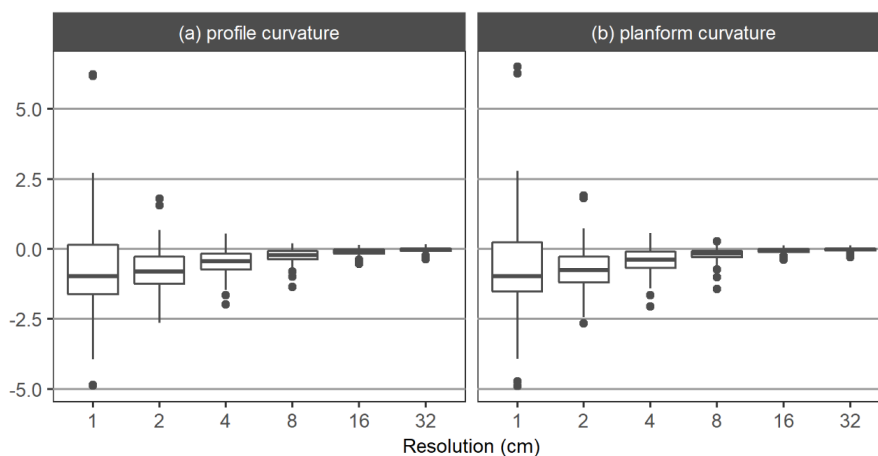


**Figure 6.** Ranges of curvature values for (a) profile curvature and (b) planform at 1-, 2-, 4-, 8-, 16- and 32-cm resolutions.

## 5. Conclusions

Three-dimensional reconstruction of coral reefs using photogrammetric techniques allows for extraction of various habitat metrics from resulting DEMs exported at different resolutions. Fractal dimension, which utilizes information on 3D surface areas obtained at different resolutions, and VRM at relatively high resolutions are the most suitable metrics for capturing the structural complexity of benthic organisms among those examined in the present study. Profile curvature and planform curvature at 1-cm resolution also capture some 3D structure of benthos. Thus, either fractal dimension or VRM obtained at 1-, 2- or 4-cm resolution, in combination with curvature obtained at 1-cm resolution, should effectively capture the 3D structure of benthic organisms. Further investigations should consider how the underlying surface topography of coral reefs affects slope and curvature values in order to adequately characterize the 3D structure of coral reef habitats.

**Supplementary Materials:** The following are available online at <http://www.mdpi.com/2072-4292/12/6/1011/s1>, Figure S1: A illustration of the GCP unit, reflective articulated triangulator (RAT), used in the present study, Figure S2: Examples of orthophotomosaics and DEMs from French Frigate Shoals (a) with *Acropora* table corals and (b) without *Acropora*. An orthophotomosaic is shown on the top. Under the orthophotomosaic, a DEM from the same model, as well as VRM and slope extracted from the DEM, at 1-cm resolution are shown on the left. The area indicated by a blue square is also shown at 1-, 2- and 4-cm resolution on the right for visualization of the DEM or the metrics at different raster cell sizes.

**Author Contributions:** Conceptualization, A.F. and J.H.R.B.; methodology, A.F. and J.H.R.B.; validation, A.F., J.H.R.B. and K.H.P.; formal analysis, A.F.; programming, A.F.; investigation, A.F., J.H.R.B. and K.H.P.; resources, J.H.R.B. and R.K.K.; data curation, A.F. and J.H.R.B.; writing—original draft preparation, A.F.; writing—review and editing, A.F., J.H.R.B., K.H.P. and R.K.K.; visualization, A.F. and K.H.P.; funding acquisition, J.H.R.B. and R.K.K. All authors have read and agreed to the published version of the manuscript.

**Funding:** This work was funded by NOAA's Office of National Marine Sanctuaries through the Papahānaumokuākea Marine National Monument, by the National Science Foundation under the CREST-PRF Award #1720706 and EPSCoR Program Award OIA #1557349 to J.H.R. Burns, and by the National Fish and Wildlife Foundation under Award # NFWF-UHH-059023 to J.H.R. Burns.

**Acknowledgments:** We thank the officers and crew of NOAA ship *Hi'ialakai* for logistic support and field assistance and Jason Leonard and Jake Asher for the collection of imagery. We also thank Sofia Ferreira Colman, Jazmin Helzer, Brittany Wells, Shane Murphy, Mia Lamirand and Brianna Craig for annotations of orthophotomosaics, and the five anonymous reviewers who improved the manuscript through their input. The scientific results and conclusions, as well as any views or opinions expressed herein, are those of the authors and do not necessarily reflect the views of NOAA or the Department of Commerce.

**Conflicts of Interest:** The authors declare no conflict of interest.

## Appendix A

**Table A1.** Regression coefficients of fixed terms in the selected models for the complexity metrics: fractal dimension, surface complexity, slope and VRM. The selected models did not include the island/atoll term as a random effect. Pseudo  $R^2$  values for the selected models are also shown.

Resolution	Model	Tabulate Corals	Branching Corals	Encrusting Corals	Mounding Corals	Algae	CCA	Hard Substrates	Rubble	Pseudo $R^2$
<b>Fractal dimension</b>										
1–32 cm	1	0.091	0.368	0.099	0.329		0.132			0.712
<b>Surface complexity</b>										
1 cm	2		1.186	0.773	4.647		0.887			0.586
2 cm	2			0.654	4.204	−0.256	0.824			0.524
4 cm	2			0.447	2.638	−0.219	0.650			0.429
8 cm	2			0.254	1.194		0.444		−1.301	0.267
16 cm	2	−0.300	−0.598		0.954	−0.247		−0.166	−1.221	0.176
32 cm	2		−0.443		1.150				−0.799	0.131
<b>Slope</b>										
1 cm	2		28.002	18.197	48.241		19.085	3.581		0.622
2 cm	2		21.628	21.376	58.140		19.878	5.260		0.546
4 cm	2			19.886	81.282		18.815	6.146	−52.780	0.429
8 cm	2				89.286				−91.458	0.257
16 cm	2		−34.571		107.099				−106.964	0.190
32 cm	2	−11.591	−47.015		104.499				−95.257	0.174
<b>VRM</b>										
1 cm	1		0.225	0.048			0.045		0.114	0.699
2 cm	1		0.214	0.076			0.055		0.103	0.737
4 cm	2	0.054	0.144	0.052	0.154		0.054			0.700
8 cm	2			0.058	0.190	−0.018	0.050			0.494
16 cm	2				0.139	−0.030	−0.019	−0.093		0.284
32 cm	2	−0.060	−0.080			−0.040		−0.030	−0.130	0.125

**Table A2.** Regression coefficients of fixed terms in the selected models for profile curvature and planform curvature. Tabulate corals, encrusting corals and rubble were never in any of the selected models so they were omitted from this table. Pseudo  $R^2$  values for the selected models and models only with the island term fitted as a random effect are also shown.

Resolution	Curvature	Model	Branching Corals	Mounding Corals	Algae	CCA	Hard Substrates	Pseudo $R^2$ (Model)	Pseudo $R^2$ (Island Term Only)
1 cm	profile	3	-10.220	23.522		4.634		0.331	0.076
	planform	3	-10.454	23.920		4.597		0.328	0.073
2 cm	profile	3	-3.649					0.235	0.193
	planform	3	-3.710					0.225	0.182
4 cm	profile	4						0.227	0.227
	planform	4						0.194	0.194
8 cm	profile	4						0.263	0.263
	planform	4						0.209	0.209
16 cm	profile	4		-1.306				0.341	0.305
	planform	4			0.270		0.220	0.365	0.357
32 cm	profile	3		-1.283				0.243	0.223
	planform	3	0.266	-0.641	0.129		0.112	0.453	0.373



## References

1. Jones, C.G.; Lawton, J.H.; Shachak, M. Organisms as ecosystem engineers. *Oikos* **1994**, *69*, 373–386. [[CrossRef](#)]
2. Jones, G.P.; Syms, C. Disturbance, habitat structure and the ecology of fishes on coral reefs. *Aust. Ecol.* **1998**, *23*, 287–297. [[CrossRef](#)]
3. Graham, N.A.J.; Nash, K.L. The importance of structural complexity in coral reef ecosystems. *Coral Reefs* **2013**, *32*, 315–326. [[CrossRef](#)]
4. Holbrook, S.J.; Brooks, A.J.; Schmitt, R.J. Variation in structural attributes of patch-forming corals and in patterns of abundance of associated fishes. *Mar. Freshw. Res.* **2002**, *53*, 1045–1053. [[CrossRef](#)]
5. Messmer, V.; Jones, G.P.; Munday, P.L.; Holbrook, S.J.; Schmitt, R.J.; Brooks, A.J. Habitat biodiversity as a determinant of fish community structure on coral reefs. *Ecology* **2011**, *92*, 2285–2298. [[CrossRef](#)]
6. Komyakova, V.; Jones, G.P.; Munday, P.L. Strong effects of coral species on the diversity and structure of reef fish communities: A multi-scale analysis. *PLoS ONE* **2018**, *13*, e0202206. [[CrossRef](#)]
7. Hunter, C.L.; Evans, C.W. Coral reefs in Kaneohe Bay, Hawaii: Two centuries of western influence and two decades of data. *Bull. Mar. Sci.* **1995**, *57*, 501–515.
8. Connell, J.H.; Hughes, T.P.; Wallace, C.C. A 30-year study of coral abundance, recruitment, and disturbance at several scales in space and time. *Ecol. Monogr.* **1997**, *67*, 461–488. [[CrossRef](#)]
9. Bellwood, D.R.; Hughes, T.P.; Folke, C.; Nyström, M. Confronting the coral reef crisis. *Nature* **2004**, *429*, 827–833. [[CrossRef](#)]
10. Loya, Y.; Sakai, K.; Yamazato, K.; Nakano, Y.; Sambali, H.; Van Woesik, R. Coral bleaching: The winners and the losers. *Ecol. Lett.* **2001**, *4*, 122–131. [[CrossRef](#)]
11. Hughes, T.P.; Kerry, J.T.; Baird, A.H.; Connolly, S.R.; Dietzel, A.; Eakin, C.M.; Heron, S.F.; Hoey, A.S.; Hoogenboom, M.O.; Liu, G.; et al. Global warming transforms coral reef assemblages. *Nature* **2018**, *556*, 492–496. [[CrossRef](#)] [[PubMed](#)]
12. Hoegh-Guldberg, O.; Mumby, P.J.; Hooten, A.J.; Steneck, R.S.; Greenfield, P.; Gomez, E.; Harvell, C.D.; Sale, P.F.; Edwards, A.J.; Caldeira, K.; et al. Coral reefs under rapid climate change and ocean acidification. *Science* **2007**, *318*, 1737–1742. [[CrossRef](#)] [[PubMed](#)]
13. Alvarez-Filip, L.; Dulvy, N.K.; Gill, J.A.; Côté, I.M.; Watkinson, A.R. Flattening of Caribbean coral reefs: Region-wide declines in architectural complexity. *Proc. R. Soc. B Biol. Sci.* **2009**, *276*, 3019–3025. [[CrossRef](#)]
14. Burns, J.H.R.; Delparte, D.; Gates, R.D.; Takabayashi, M. Integrating structure-from-motion photogrammetry with geospatial software as a novel technique for quantifying 3D ecological characteristics of coral reefs. *PeerJ* **2015**, *3*, e1077. [[CrossRef](#)] [[PubMed](#)]
15. Burns, J.H.R.; Delparte, D.; Kapon, L.; Belt, M.; Gates, R.D.; Takabayashi, M. Assessing the impact of acute disturbances on the structure and composition of a coral community using innovative 3D reconstruction techniques. *Methods Oceanogr.* **2016**, *15*, 49–59. [[CrossRef](#)]
16. Leon, J.X.; Roelfsema, C.M.; Saunders, M.I.; Phinn, S.R. Measuring coral reef terrain roughness using ‘Structure-from-Motion’ close-range photogrammetry. *Geomorphology* **2015**, *242*, 21–28. [[CrossRef](#)]
17. Young, G.C.; Dey, S.; Rogers, A.D.; Exton, D. Cost and time-effective method for multi-scale measures of rugosity, fractal dimension, and vector dispersion from coral reef 3D models. *PLoS ONE* **2017**, *12*, e0175341. [[CrossRef](#)]
18. Ferrari, R.; Bryson, M.; Bridge, T.; Hustache, J.; Williams, S.B.; Byrne, M.; Figueira, W. Quantifying the response of structural complexity and community composition to environmental change in marine communities. *Glob. Chang. Biol.* **2016**, *22*, 1965–1975. [[CrossRef](#)]
19. Burns, J.H.R.; Fukunaga, A.; Pascoe, K.H.; Runyan, A.; Craig, B.K.; Talbot, J.; Pugh, A.; Kosaki, R.K. 3D habitat complexity of coral reefs in the Northwestern Hawaiian Islands is driven by coral assemblage structure. *Limnol. Oceanogr.* **2019**, *64*, 61–67. [[CrossRef](#)]
20. Fukunaga, A.; Burns, J.H.R.; Craig, B.K.; Kosaki, R.K. Integrating three-dimensional benthic habitat characterization techniques into ecological monitoring of coral reefs. *J. Mar. Sci. Eng.* **2019**, *7*, 27. [[CrossRef](#)]
21. Walbridge, S.; Slocum, N.; Pobuda, M.; Wright, D.J. Unified geomorphological analysis workflows with Benthic Terrain Modeler. *Geosciences* **2018**, *8*, 94. [[CrossRef](#)]
22. Horn, B.K.P. Hill shading and the reflectance map. *Proc. IEEE* **1981**, *69*, 14–47. [[CrossRef](#)]

23. Sappington, J.M.; Longshore, K.M.; Thompson, D.B. Quantifying landscape ruggedness for animal habitat analysis: A case study using bighorn sheep in the Mojave Desert. *J. Wildl. Manag.* **2007**, *71*, 1419–1426. [[CrossRef](#)]
24. Zevenbergen, L.W.; Thorne, C.R. Quantitative analysis of land surface topography. *Earth Surf. Process. Landf.* **1987**, *12*, 47–56. [[CrossRef](#)]
25. Beijbom, O.; Edmunds, P.J.; Roelfsema, C.; Smith, J.; Kline, D.I.; Neal, B.P.; Dunlap, M.J.; Moriarty, V.; Fan, T.-Y.; Tan, C.-J.; et al. Towards automated annotation of benthic survey images: Variability of human experts and operational modes of automation. *PLoS ONE* **2015**, *10*, e0130312. [[CrossRef](#)] [[PubMed](#)]
26. R Core Team. *R: A Language and Environment for Statistical Computing*, v. 3.5.3; R Foundation for Statistical Computing: Vienna, Austria, 2019.
27. Pebesma, E.J.; Bivand, R.S. Classes and methods for spatial data in R. *R News* **2005**, *5*, 9–13.
28. Bivand, R.S.; Pebesma, E.; Gómez-Rubio, V. *Applied Spatial Data Analysis with R*, 2nd ed.; Springer: New York, NY, USA, 2013.
29. Hijmans, R.J. Raster: Geographic Data Analysis and Modeling. R Package Version 2.9-5. 2019. Available online: <https://CRAN.R-project.org/package=raster> (accessed on 19 November 2019).
30. Bivand, R.; Rundel, C. Rgeos: Interface to Geometry Engine—Open Source (GEOS). R Package Version 0.4-3. 2019. Available online: <https://CRAN.R-project.org/package=rgeos> (accessed on 19 November 2019).
31. Pinheiro, J.; Bates, D.; DebRoy, S.; Sarkar, D.; R Core Team. NLME: Linear and Nonlinear Mixed Effects Models. R Package Version 3.1-137. 2018. Available online: <https://CRAN.R-project.org/package=nlme> (accessed on 26 November 2019).
32. Fox, J.; Weisberg, S. *An R Companion to Applied Regression*, 3rd ed.; Sage: Thousand Oaks, CA, USA, 2019.
33. Basillais, É. Coral surfaces and fractal dimensions: A new method. *Comptes Rendus Acad. Sci.* **1997**, *320*, 653–657. [[CrossRef](#)]
34. Reichert, J.; Backes, A.R.; Schubert, P.; Wilke, T. The power of 3D fractal dimensions for comparative shape and structural complexity analyses of irregularly shaped organisms. *Methods Ecol.* **2017**, *8*, 1650–1658. [[CrossRef](#)]
35. Bradbury, R.H.; Reichelt, R.E. Fractal dimension of a coral reef at ecological scales. *Mar. Ecol. Prog. Ser.* **1983**, *10*, 169–171. [[CrossRef](#)]
36. Risk, M.J. Fish diversity on a coral reef in the Virgin Islands. *Atoll Res. Bull.* **1972**, *153*, 1–4. [[CrossRef](#)]
37. Kundby, A.; LeDrew, E. Measuring structural complexity on coral reefs. In Proceedings of the American Academy of Underwater Sciences 26th Symposium, Coral Gables, FL, USA, 9–10 March 2007; Pollock, N.W., Godfrey, J.M., Eds.; AAUS: Dauphin Island, AL, USA, 2007; pp. 181–188.
38. Fukunaga, A.; Kosaki, R.K.; Hauk, B.B. Distribution and abundance of the introduced snapper *Lutjanus kasmira* (Forsskål, 1775) on shallow and mesophotic reefs of the Northwestern Hawaiian Islands. *Bioinvasions Rec.* **2017**, *6*, 259–268. [[CrossRef](#)]
39. Blaga, L. Aspects regarding the significance of the curvature types and values in the studies of geomorphometry assisted by GIS. *Ann. Univ. Oradea Ser. Geogr.* **2012**, *XXII*, 327–337.



© 2020 by the authors. Licensee MDPI, Basel, Switzerland. This article is an open access article distributed under the terms and conditions of the Creative Commons Attribution (CC BY) license (<http://creativecommons.org/licenses/by/4.0/>).